J Mater Sci (2007) 42:9920–9926
DOI 10.1007/s10853-007-2098-4

Mass spectroscopic measuring of $SiCl_n$ (n = 0–2) radicals in $SiCl_4$ RF glow discharge plasma

Zhaokui Wang · Yanhui Lou

Received: 1 December 2006 / Accepted: 13 August 2007 / Published online: 6 September 2007

Abstract The relative densities of $SiCl_n$ ($n = 0$–2) in $SiCl_4$ radio frequency (rf) glow discharge plasma are measured by mass spectrometry. The effects of discharge parameters, i.e., rf power, discharge pressure, substrate temperature, and $SiCl_4$ flow rate on the relative densities of $SiCl_n$ ($n = 0$–2) are investigated in detail. An optimum configuration of discharge parameters (low rf power, high discharge pressure, low substrate temperature, and low flow rate), which enhanced the formation of $SiCl_n$ ($n = 0$–2) radicals, is searched by a great deal of measurements and discussions. In the optimum configuration of discharge parameters, we measure the spatial distribution of $SiCl_n$ ($n = 0$–2) radicals in the most optimized plasma parameters. The experimental results reveal that Si and SiCl may be the dominant precursors in forming the thin film.

Introduction

Silicon tetrachloride ($SiCl_4$), as one of the widely used gases, has been proved effective in the chemical vapor deposition (CVD) for polycrystalline silicon (poly-Si) and related thin films for manufacturing solar cells, thin film transistors, and patterning small structures such as Si-based metal-oxide-semiconductor (MOS) device [1–8]. In previous work, we have deposited poly-Si films using $SiCl_4/H_2$ gases by plasma-enhanced chemical vapor deposition (PECVD) technique and obtained the poly-Si films with the deposition rate over 3.0 Å/s without deterioration of the optoelectronic properties [9, 10]. To improve deposition rate and film quality, it is important to clarify the deposition mechanism of poly-Si films.

A great deal of work has been carried out on the characterization of deposited material from both a chemical and a physical point of view, while less has been directed to the study on deposition mechanism of the film. The growing model and the deposition process of the films from $SiCl_4$ are relatively more complex because of the presence of an etching mechanism that affects the growth rate [8]. It is generally accepted that the major precursors of films' deposition are $SiCl_n$ ($n = 0$–2) radicals in plasma, while $SiCl_3$, Cl, and Cl_2 are primary etchants of films [11–14]. Therefore it is important to provide experiment data on these species' gas phase densities under typical deposition conditions in order to improve the understanding of the plasma processes.

The diagnosis and measurement of the primary particles in deposition and etching process make it better to understand the mechanism of film deposition and etching, which can improve the qualities and characteristics of films. In earlier studies, the $SiCl_n$ ($n = 0$–2) species concentration has been measured by optical emission spectroscopy and broadband absorption spectroscopy diagnostic techniques [15–18]. These optical spectroscopy diagnostic techniques are powerful for measuring the neutral radicals in plasma with higher sensitivity and spatial resolution. However, the exciting and emitting spectra of these radicals always cover a very wide range, generally from the ultraviolet rays to the infrared rays, these spectra have to be measured by a different spectrometer. In other words, it is difficult for only one spectroscopy setup to detect simultaneously all radicals in plasma. Mass spectrometry is a simple and useful diagnostic technique and it can measure all radicals in plasma if it has a large mass range. And it is superior to

Z. K. Wang (✉) · Y. H. Lou
Department of Physics, Henan Normal University, Xinxiang 453007, P.R. China
e-mail: zhaokuiwang@163.com

optical spectroscopic diagnosis in identification of plasma components and measurement of particles concentration in plasma vapor reaction, and interaction between plasma and surface. However, it must be operated under a high vacuum environment due to its particular conformation and operation principle. This makes it detect, only those gas species sampled from a fixed position of plasma bulk, such as aperture of discharge chamber wall and discharge electrodes. Until now, no space property in $SiCl_4$ plasma has been measured by means of mass spectroscopy analysis.

Presently, we propose and establish a movable gas sampling apparatus, which is suitable for mass spectroscopic sampling in our laboratory [19]. Using the movable apparatus, we can diagnose plasma states and analyze gas species properties at any sampling position in plasma. In this article, we focused on the effects of plasma parameters, such as radio frequency (rf) power, discharge pressure, substrate temperature, and $SiCl_4$ flow rate on $SiCl_n$ (n = 0–2) densities for searching an optimum parameter configuration of discharge plasma. Furthermore, we measured the spatial distributions of $SiCl_n$ (n = 0–2) radicals in $SiCl_4$ radio frequency (rf) (13.56 MHz) glow discharge plasma.

Experiments and methods

Experimental arrangements

The experimental setup is shown schematically in Fig. 1. The discharge chamber was equipped with two parallel plate electrodes made of stainless steel. The $SiCl_4$ glow discharge in the chamber was generated by a capacitively coupled rf power source and confined in the space between the parallel electrodes with a gap of 30 mm. The glass was used for the substrate. Other technology parameters variations were the rf power (2–50 W, corresponding to power densities of 0.02–0.5 W cm^{-2}), the discharge pressure (10–50 Pa), the $SiCl_4$ flow rate (7–20.5 SCCM), and substrate temperature (25–400 °C). The mass spectrometry sampling tube was located at 1 mm below substrate. The sampled gas species from plasma region were leaked into the ionization chamber of residual gas analyzer (RGA) via the movable gas sampling apparatus. The mass spectroscopy signals of the sampled gas species were detected by RGA (SRS RGA–100) with a minimum detectable partial pressure of 6.7×10^{-12} Pa.

Four series of experiments were designed to study the effects of rf power, discharge pressure, substrate temperature, and $SiCl_4$ flow rate on the relative densities of $SiCl_n$ (n = 0–2) in $SiCl_4$ plasma. In each series of measurements, only one of the parameters was varied and the rest were kept unchanged.

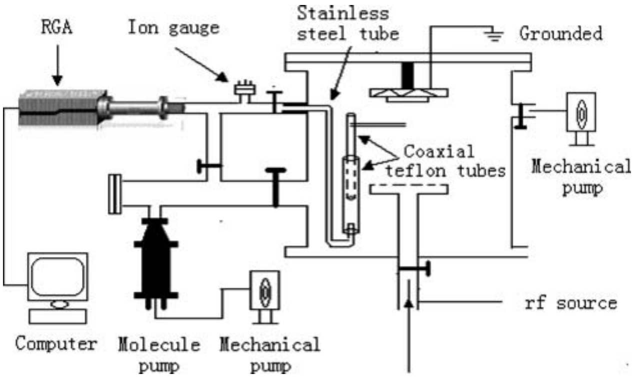

Fig. 1 Schematic of experimental apparatus for online mass spectroscopic analysis of $SiCl_4$ plasma

Calculation methods

The mass spectroscopic signals $S^n_{\mathrm{off}}(Ee)$ and $S^n_{\mathrm{on}}(Ee)$ of $SiCl_n^+$ (n = 0–2) were measured by RGA with discharge off and on at a certain electron energy (Ee), respectively. $S^n_{\mathrm{on}}(Ee)$ can be expressed as following [20]:

$$S^n_{\mathrm{on}}(Ee) = S^n_{\mathrm{ion}} + S^n(Ee) + (1-f)S^n_{\mathrm{off}}(Ee) \tag{1}$$

where, $S^n(Ee)$ was the mass spectroscopy signals of $SiCl_n$ (n = 0–2) radicals created and sampled from glow discharges chamber and ionized at Ee in RGA chamber, S^n_{ion} was ion signals of $SiCl_n^+$ (n = 0–2) created in the discharge chamber and leaked into the RGA, and f was the depletion fraction of $SiCl_4$.

The leakage ion signals were so weak to be detected though the RGA is set at the maximum sensitivity, because most of the leaked ions collided with the wall of long and thin gas sampling tube and was absorbed by it. So Eq. 1 can be simplified as following:

$$S^n_{\mathrm{on}}(Ee) = S^n(Ee) + (1-f)S^n_{\mathrm{off}}(Ee) \tag{2}$$

Despite the depletion fraction of $SiCl_4$ is a constant under a certain discharge condition and sampling position, all the signals of $S^n_{\mathrm{off}}(Ee)$, $S^n_{\mathrm{on}}(Ee)$, and $S^n(Ee)$ are changing with the change of electron energy because the ionization cross section of $SiCl_n$ (n = 0–2) and dissociation ionization cross section of $SiCl_4$ are a function of electron energy. Thus the Eq. 2 can be changed as following:

$$S^n_{\mathrm{on}}(Ee) = \alpha_n(Ee)\,S^n_0 + (1-f)\,S^n_{\mathrm{off}}(Ee) \tag{3}$$

where, $\alpha_n(Ee)$ was defined as

$$\alpha_n(Ee) = \sigma_n(Ee)/\sigma_{n\,\max}(E^n_0) \tag{4}$$

$\alpha_n(Ee)$ and $\sigma_{n\,\max}(E^n_0)$ were the ionization cross section at the electron energy (Ee) and the maximum ionization cross section corresponding to the certain electron energy (E^n_0)

for each $SiCl_n$ (n = 0–2), respectively. S_0^n was defined as the mass spectroscopic signal of the electron energy E_0^ncorresponding to the maximum ionization cross section for each $SiCl_n$ (n = 0–2) radicals. Furthermore, Eq. 3 can be simplified as following:

$$C_1^n = -S_0^n + f\,C_2^n \tag{5}$$

where $C_1^n = (S_{\mathrm{off}}^n(E_e) - S_{\mathrm{on}}^n(E_e))/\alpha_n(E_e)$, $C_2^n = S_{\mathrm{off}}^n(E_e)/\alpha_n(E_e)$.

According to Eq. 5, the slope of a fit straight line of C_1^n versus C_2^n was just the value of depletion fraction f. The depletion fraction of $SiCl_4$ was deduced from the SiCl and $SiCl_2$ mass spectrometric signals, respectively. The values of ionization cross sections of $SiCl_n$ (n = 1,2) radicals were calculated using the theoretical models of Joshipura [21].

Define $S^n(E_{e0})$ as the S^n at a certain electron energy E_{e0}, $S^n(E_{e0})$ can be expressed as following,

$$S^n(E_{e0}) = S_{\mathrm{on}}^n(E_{e0}) - (1-f)\,S_{\mathrm{off}}^n(E_{e0})\,. \tag{6}$$

Obviously, S^n (E_{e0}) was characterized as the relative densities of $SiCl_n$ (n = 0–2) in $SiCl_4$ plasma. We calculated the relative densities of $SiCl_n$ (n = 0–2) by Eq. 6 using the average value of depletion fractions deduced from the SiCl and $SiCl_2$ mass spectrometric signals. For higher accuracy, the $SiCl_n$ (n = 0–2) radical relative densities were calculated at E_{e0} = 90 eV.

Results and discussion

The effects of plasma parameters

rf Power

Figure 2 shows the change of $SiCl_4$ depletion fraction (deduced by SiCl and $SiCl_2$ MS signals, respectively) with the increasing of rf power. It is obvious that the depletion fraction of $SiCl_4$ increases remarkably by adding rf power. As reported previously, the plasma gas phase reaction depends strongly on the rf power [20]. The electron density and the electron temperature increase with the increasing rf power. The high electron density and electron temperature promote the ionization and dissociation of $SiCl_4$, which result in the larger depletion fraction of $SiCl_4$.

The dependences of Si, SiCl, and $SiCl_2$ relative densities on rf power are shown in Fig. 3a–c, respectively. As like the trend of $SiCl_4$ depletion fraction, Si relative density increases remarkably with the adding of the rf power when the rf power is less than 20 W. It remains almost a constant value while further increasing the rf power. Contrarily, the relative densities of SiCl and $SiCl_2$ decrease with adding of the rf power.

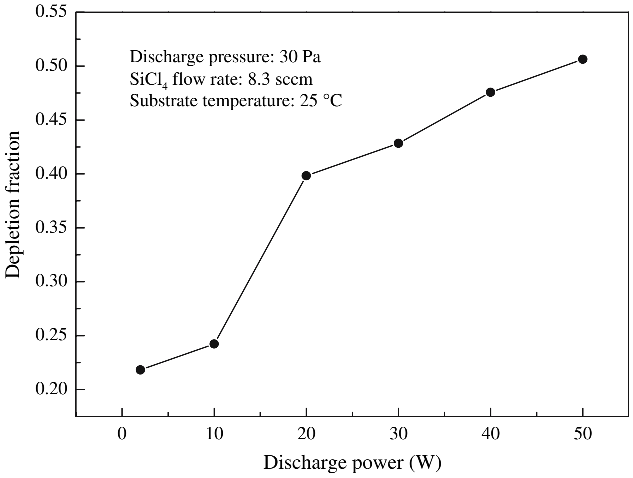

Fig. 2 The depletion fraction of $SiCl_4$ versus rf power

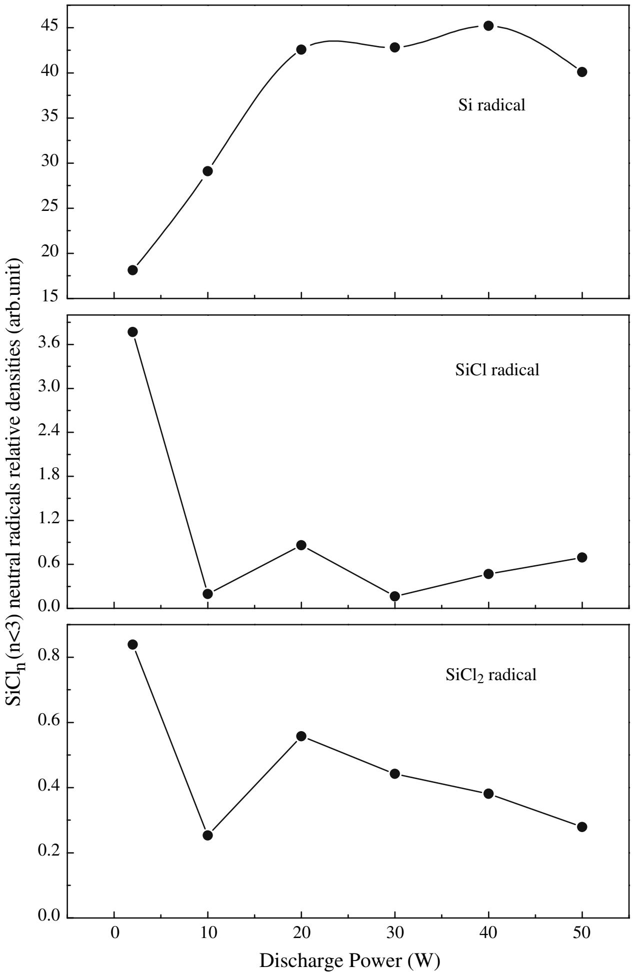

Fig. 3 **(a–c)** The dependences of Si, SiCl, and $SiCl_2$ relative densities on rf power under the discharge pressure 30 Pa, $SiCl_4$ flow rate 8.3 SCCM and substrate temperature 25 °C

Although the $SiCl_4$ depletion fraction increases with the rf power, the ionization process and dissociation process both result in the depletion of $SiCl_4$. Particularly, the electron energy resulting in the formation of $SiCl_n^+$ by impacting $SiCl_4$ molecule is larger than that resulting in the formation of $SiCl_n$ by impacting $SiCl_4$ molecule. Under lower rf power, the average electron energy and the electron density have smaller values, and the dissociation of $SiCl_4$ plays an important role, which enhances the formation of $SiCl_n$ radicals. With further increasing of rf power, the average electron energy also increases, which results in a dominant ionization process in $SiCl_4$ plasma. What is more, the higher rf power promotes a secondary reaction between energetic electrons and $SiCl_n$ radicals, which result in the formation of $SiCl_{n-1}$ and $SiCl_{n-1}^+$. This might be the reason why the relative densities of SiCl and $SiCl_2$ have smaller values at higher rf power and the relative density of SiCl is larger than that of $SiCl_2$. Si radical is formed mostly by the plasma reaction of $e^- + SiCl_4 \rightarrow Si + 2Cl_2 + e^-$ and $e^- + SiCl_n \rightarrow Si + nCl + e^-$. With the increase of rf power, the average electron energy is also increased, which results in larger probability of the former plasma reaction. Therefore, Si relative density increases remarkably by with adding the rf power. When the rf power is larger than 20 W, the relative densities of SiCl and $SiCl_2$ have not remarkably changed, and Si relative density is almost a constant value when the rf power is larger than 20 W.

Discharge pressure

The depletion fraction dependence of the discharge pressure in $SiCl_4$ plasma is shown in Fig. 4. By increasing the discharge pressure from 10 Pa to 50 Pa, the $SiCl_4$ depletion fraction keeps almost constant values in the whole experimental discharge pressure. This means that the $SiCl_4$ depletion fraction does not depend strongly on the discharge pressure in plasma.

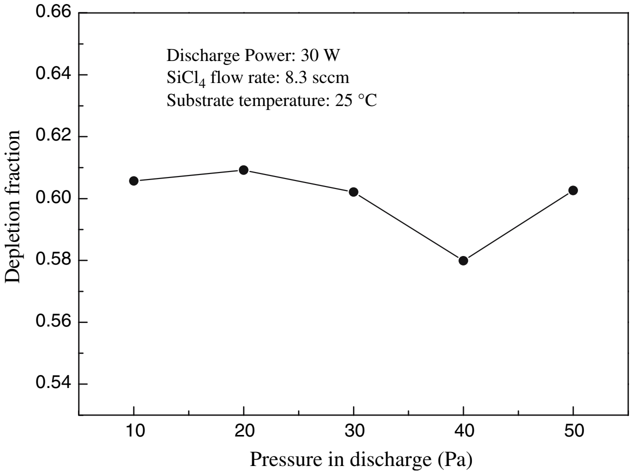

Fig. 4 The depletion fraction of $SiCl_4$ versus discharge pressure

The dependences of Si, SiCl, and $SiCl_2$ relative densities on discharge pressure are shown in Fig. 5a–c, respectively. Si relative density increases almost linearly by adding the discharge pressure from 10 Pa to 50 Pa. With the increasing discharge pressure, there will be increasing $SiCl_4$ molecules and $SiCl_4$ depletion fraction keeps almost constant values in the whole experimental discharge pressure as depicted above, which enhances the formation of $SiCl_n$ radicals. However, the change of relative densities of SiCl and $SiCl_2$ do not have a clear trend of the increasing discharge pressure from 10 Pa to 50 Pa. The discharge pressure is perhaps the most misunderstood and ill-treated parameter of glow discharge. Detailed studies are needed for clarifying the effects of discharge pressure on relative densities of $SiCl_n$ (n = 0–2).

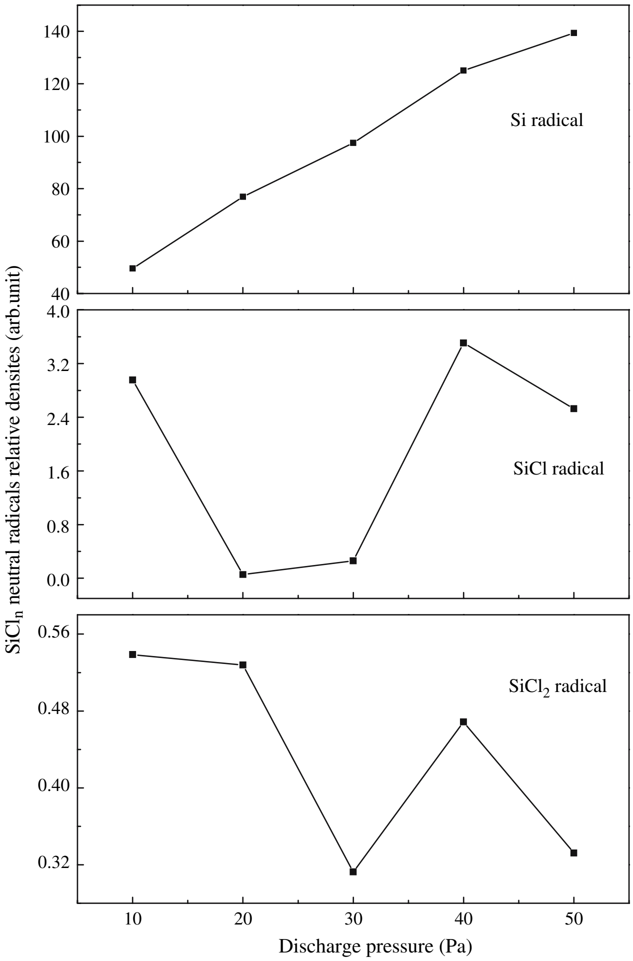

Fig. 5 (**a**–**c**) The dependences of Si, SiCl, and $SiCl_2$ relative densities on discharge pressure under the rf power 30 W, $SiCl_4$ flow rate 8.3 SCCM, and substrate temperature 25 °C

$SiCl_4$ flow rate

Figure 6 shows the depletion fraction of $SiCl_4$ versus flow rate of $SiCl_4$. It is obvious that the depletion fraction of $SiCl_4$ decreases with the increase of $SiCl_4$ flow rate in the range of 7–20.5 SCCM. This may be relative with the residence time of the $SiCl_4$ molecule in plasma. As we all know, the gas flow rate (F) decides the average residence time (t) of one $SiCl_4$ molecule in plasma. The average residence time (t) decides the probability of dissociation of one $SiCl_4$ molecule and the dissociation radicals, which are primary precursors of depositing films, and also the depletion extent of $SiCl_4$ in plasma. When chamber pressure and discharge power remain constant, the more t is long, the more the depletion fraction of $SiCl_4$ is large, and there will be more react radicals in $SiCl_4$ plasma. What is more, t is related to not only the flow rate F, but also some other factors. Under the experimental conditions of chamber pressure P, plasma bulk volume V (space bulk between two electrodes) and initial pressure P_0, the variation tendency of t can be expressed as following:

$$t \propto PV/P_0\ F, \tag{7}$$

When P, V, and P_0 are all maintained as constants, t decreases with the increase of flow rate F. That is why the depletion fraction of $SiCl_4$ decreases with the increase of $SiCl_4$ flow rate under chamber pressure and discharge power maintained constant.

Figure 7a–c shows the Si, SiCl, and $SiCl_2$ densities versus flow rate of $SiCl_4$, respectively. From Fig. 7, we can see that Si density decreases with the increase of flow rate in the range of 7–17 SCCM, then slightly increases with the increase of flow rate in the range of 17–20.5 SCCM; and both of $SiCl_n$ (n = 1,2) densities decrease with the increase of flow rate in the range of 7–13 SCCM, then slightly increases with the increase of flow rate in the range of 13–20.5 SCCM.

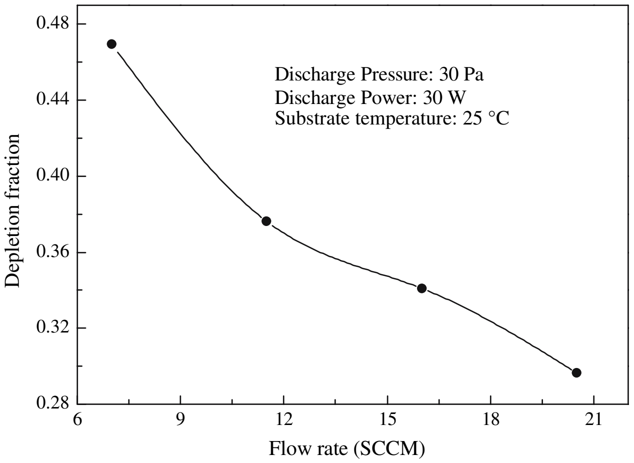

Fig. 6 The depletion fraction of $SiCl_4$ versus $SiCl_4$ flow rate

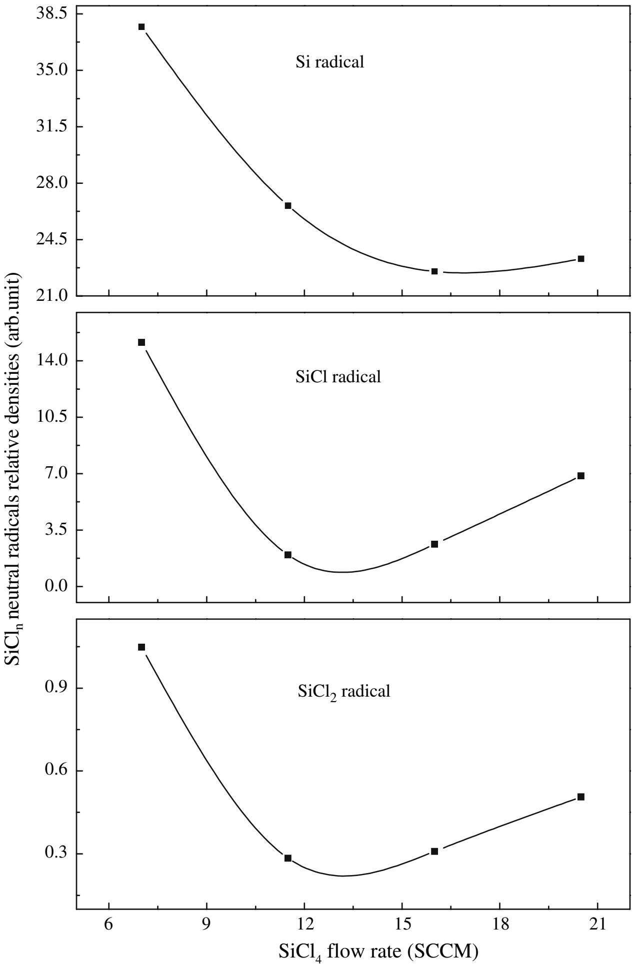

Fig. 7 (**a–c**) The dependences of Si, SiCl, and $SiCl_2$ relative densities on $SiCl_4$ flow rate under the discharge pressure 30 Pa, rf power 30 W, and substrate temperature 25 °C

As discussed above, with the increase of $SiCl_4$ flow rate, the residence time of $SiCl_4$ molecule becomes short, the depletion fraction of $SiCl_4$ becomes small, and there will be less reactive radicals, such as $SiCl_n$ (n = 0–2) in $SiCl_4$ plasma. On the other hand, due to the higher flow rate, the negative ions confined in the discharge volume by the plasma potential are swept away from the reaction region by the gas flow forming a lower steady-state density.21This is also the reason why reduced $SiCl_n$ (n = 0–2) densities are observed with the increase of $SiCl_4$ flow rate.

Substrate Temperature

Figure 8 shows the change of $SiCl_4$ depletion fraction as a function of substrate temperature (25–400 °C). And the dependences of Si, SiCl, and $SiCl_2$ relative densities on

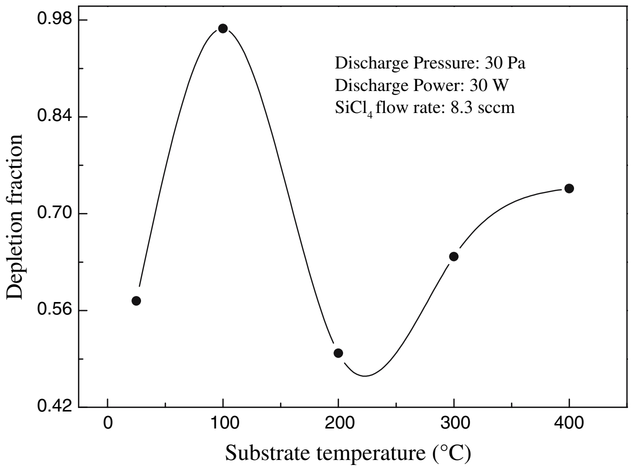

Fig. 8 The depletion fraction of $SiCl_4$ versus substrate temperature

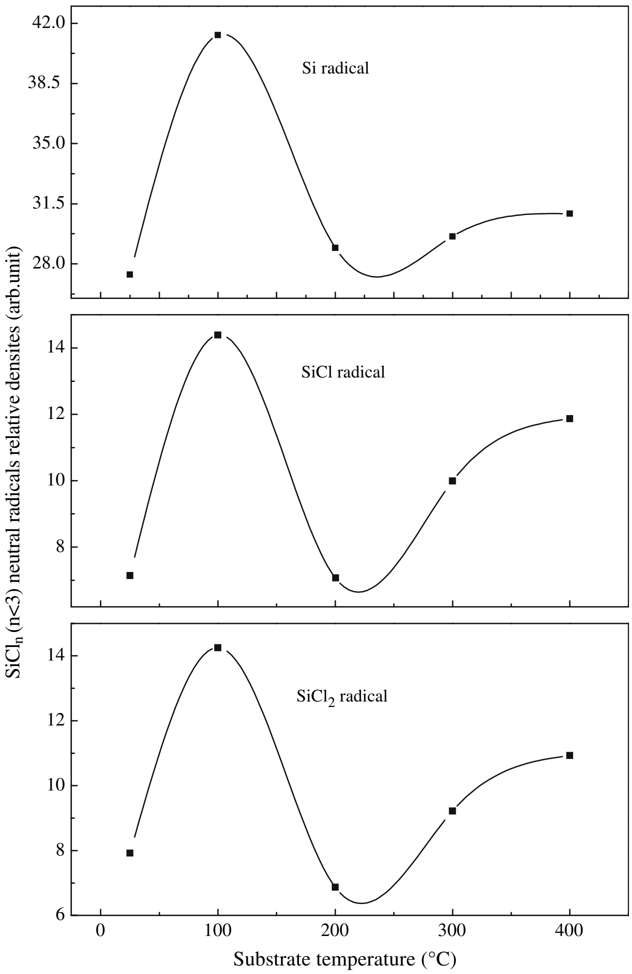

Fig. 9 (**a–c**) The dependences of Si, SiCl, and $SiCl_2$ relative densities on substrate temperature under the discharge pressure 30 Pa, rf power 30 W, and $SiCl_4$ flow rate 8.3 SCCM

substrate temperature are shown in Fig. 9a–c, respectively. As shown in Figs. 8 and 9, $SiCl_4$ depletion fraction and the relative densities of $SiCl_n$ ($n = 0$–2) have the same trend in the whole experimental temperature. At 100 °C, the relative densities of $SiCl_n$ ($n = 0$–2) both have peak values. On the other hand, the relative densities of $SiCl_n$ ($n = 0$–2) both have values at the temperature slightly higher than 200 °C.

From Figs. 3, 5, 7, and 9, we can also see that the relative density of Si is almost one order magnitude higher than that of SiCl, and two order magnitudes higher than that of $SiCl_2$. In $SiCl_4$ plasma, the ionization fraction of $SiCl_4$ is very small, the primary components in plasma are neutral radicals, such as $SiCl_n$ ($n = 0$–3) radicals. Due to a broad distribution of electron energy in plasma, there exists secondary electron collision with $SiCl_n$ ($n = 1$–3) radicals. That is the reason why there are more Si and SiCl radicals in $SiCl_4$ plasma.

Spatial distribution of $SiCl_n$ ($n = 0$–2) radicals

As discussed above, the relative densities of $SiCl_n$ ($n = 0$–2) in $SiCl_4$ plasma were dependent strongly on rf power, discharge pressure, substrate temperature, and $SiCl_4$ flow rate. From the experimental results, we can see that low rf power, high discharge pressure, low substrate temperature, and low flow rate is contributed to the formation of $SiCl_n$ ($n = 0$–2) radicals. So, we measure the spatial distribution of $SiCl_n$ ($n = 0$–2) radicals in the following plasma parameters: chamber pressure 20 Pa, substrate temperature 25 °C, rf power 30 W (corresponding to power densities of 0.3 W cm^{-2}), and $SiCl_4$ flow rate 5.8 SCCM.

Figure 10a, b shows the axial and radial orientation distributions of $SiCl_n$ ($n = 0$–2) relative densities, respectively. It is obvious that the relative densities of the $SiCl_n$ ($n = 0$–2) radicals have peak values along the axial orientation also the radial orientation. The experimental results demonstrate that the relative densities of the $SiCl_n$ ($n = 0$–2) radicals have peak values at the position of 10 mm above the rf powered electrode along the axial orientation; the relative densities of the Si and $SiCl_n$ ($n = 1,2$) radicals have peak values at the position of 27 mm and 7 mm away from the axis along the radial orientation, respectively.

From Fig. 10a, b, we can also see that Si is the most abundant radical in $SiCl_4$ plasma, SiCl is secondary, and $SiCl_2$ is less than SiCl. Generally speaking, in the whole $SiCl_4$ plasma space, the relative density of Si is one order of magnitude higher than that of SiCl, and the relative density of SiCl is several times higher than that of $SiCl_2$. This reveals that Si and SiCl may be the dominant precursors in forming the poly-Si film.

These measured spatial distributions of $SiCl_n$ ($n = 0$–2) radicals can provide useful data for the spatial reaction process research in $SiCl_4$ plasma and understanding the

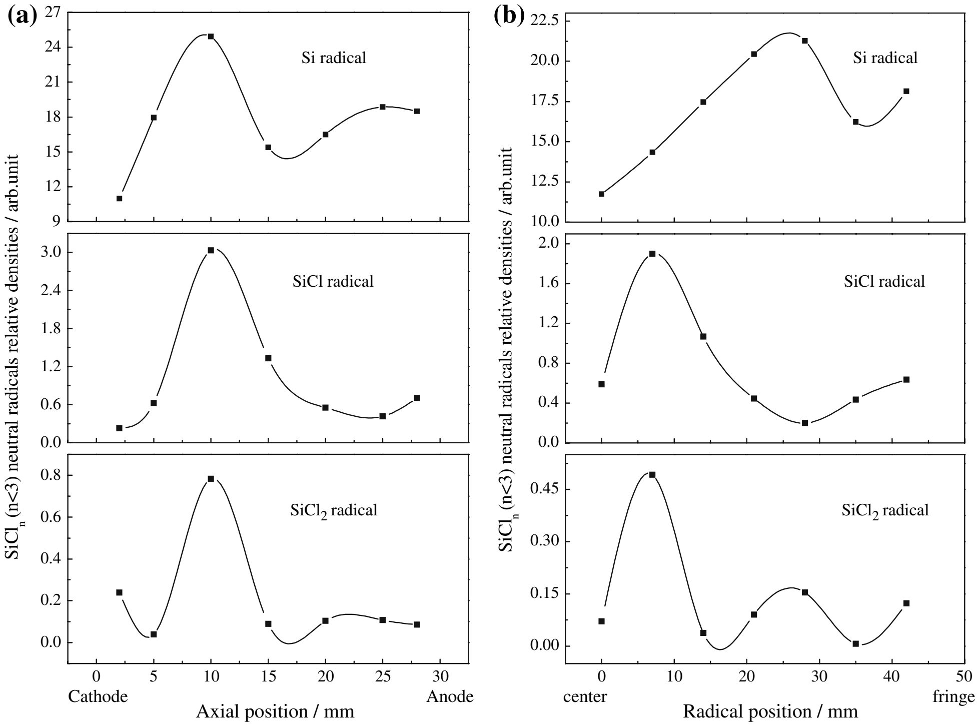

Fig. 10 (**a**) The axial distribution of SiCl$_n$ (n = 0–2) radicals relative densities; (**b**) The radical distribution of SiCl$_n$ (n = 0–2) radicals relative densities

deposition mechanism of poly-Si thin films. Further research of SiCl$_n$ (n = 0–2) radial orientation distribution for seeking a suitable deposition condition is beneficial of improving the uniformity of thin films.

Conclusions

In summary, we measured the relative densities of SiCl$_n$ (n = 0–2) radicals in SiCl$_4$ radio frequency (rf) glow discharge plasma was measured by mass spectrometry, and investigated in detail the effects of rf power, discharge pressure, substrate temperature, and SiCl$_4$ flow rate on the relative densities of SiCl$_n$ (n = 0–2) radicals. The experimental results demonstrated that the relative densities of SiCl$_n$ (n = 0–2) radicals were strongly dependent on these discharge parameters, and low rf power, high discharge pressure, low substrate temperature, and low flow rate was contributed to the formation of SiCl$_n$ (n = 0–2) radicals. Furthermore, we measure the spatial distribution of SiCl$_n$ (n = 0–2) radicals in the most optimized plasma parameters. It reveals that Si and SiCl may be the dominant precursors in forming the poly-Si film.

Acknowledgements This work is supported by the State Key Developments Program for Basic Research of China (Grant No. G2000028208). The authors would like to thank Professor K. N. Joshipura for calculating the ionization cross sections $\alpha_n(Ee)$ of SiCl$_n$ (n = 1,2) radicals.

References

1. Shirai H, Fukai C, Sakuma Y, Moriya Y (2000) J Non-Cryst Solids 266:131
2. Liu H, Jung S, Fujimura Y, Fukai C (2001) Jpn J Appl Phys 40:44
3. Cicala G, Capezzuto P, Bruno G (2001) Thin Solid Films 383:203
4. Lin KX, Lin XY, Chi LF, Yu CY, Yao RH, Yu YP (2003) Chin Phys 12:1009
5. Chen KJ, Huang XF, Xu J (2001) Chin Phys 10:748
6. Kunihide T, Takuya M, Hiroshi H (1991) Jpn J Appl Phys 30:L1208
7. Akihiro K, Naoki K, Kenichi O, Toshio G (1993) Jpn J Appl Phys 32:L543
8. Yoshitaka N, Koichi K, Toshihiko M, Makiko K, Katsuhiko H, Hironobu U, Atsushi M, Hideki M (2000) J Appl Phys 88:5437
9. Lin XY, Huang CJ, Lin KX, Yu YP, Yu CY, Chi LF (2003) Chin Phys Lett 20:1879
10. Huang R, Lin XY, Yu YP, Lin KX, Wei JH, Yu CY, Wang ZK (2004) Chin Phys Lett 21:1168
11. Bruno G, Capezzuto P, Cicala G (1987) J Appl Phys 62:2050
12. Tang YS, Wilkinson CDW (1998) Appl Phys Lett 58:2898
13. Sakai T, Sakai A, Okano H (1993) Jpn J Appl Phys 32:3089
14. Cunge G (2004) J Appl Phys 96:4578
15. Sansa RS, Ronn AM (1985) Chem Phys 96:183
16. Washida N, Matsumi Y, Hayashi T (1985) J Chem Phys 83:2769
17. Neill JO', Singh J (1994) J Appl Phys 76:5967
18. Booth JP, Cunge G, Neuilly F (1998) Plasma Sources Sci Technol 7:423
19. Wang ZK, Lou YH, Lin KX, Lin XY (2007) Int J Mass Spec 261:25
20. Robertson R, Gallagher A (1986) J Appl Phys 59:3402
21. Joshipura KN, Minaxi V, Limbachiya CG, Antony BK (2004) Phys Rev A 69:022705